Optical and EPR studies of Fe^{3+} doped tin oxide thin films by spray pyrolysis

M. C. RAO[a*], K. RAVINDRANADH[a], R. V. S. S. N. RAVIKUMAR[b]
[a]*Department of Physics, Andhra Loyola College, Vijayawada-520008, India*
[b]*Department of Physics, Acharya Nagarjuna University, Nagarjuna Nagar-522510, India*

In the present study, Fe^{3+} doped SnO_2 thin films were synthesized by chemical spray pyrolysis method. The as-prepared samples were characterized by powder X-ray diffraction (XRD), optical and electron paramagnetic resonance (EPR) studies to collect the information about the crystal structure and the local site symmetry of doped Fe^{3+} ions in the SnO_2 lattice. The powder XRD data revealed that the crystal structure belongs to a tetragonal rutile phase of SnO_2 and its lattice cell parameters were evaluated. The average crystallite size was found to be around 23 nm. The EPR spectrum revealed a resonance signal at around g = 2.07, which can be ascribed to iron ions into the host lattice at a distorted octahedral site symmetry and also confirmed from the optical absorption studies.

(Received December 10, 2016; accepted April 5, 2018)

Keywords: SnO_2, Thin films, Spray pyrolysis, Powder X-ray diffraction, Optical and EPR

1. Introduction

Tin oxide (SnO_2) is a special oxide material because it has a low electrical resistance with high optical transparency in the visible range [1, 2]. Due to the unique properties and abundance, SnO_2 is extensively studied as cost-effective metal oxide semiconductor for potential solutions of environmental problems [3]. The suitability and tunability of band structure of SnO_2, as well as the chemical, thermal stability and non-toxicity, make it an appropriate material for liquid crystal displays, gas sensors, flat panel display and heat reflectors in solar cells. For most of these applications, SnO_2 is valuable to use in the form of thin films and it has interesting properties for several applications [4].

Thin films based semiconducting materials are very fascinating and can be used in many applications as coating materials, heat mirrors, catalysis in optoelectronic, plasma devices and electrochromic devices etc. [5]. There is a great demand and usage for transparent conductive oxides (TCOs) based semiconducting oxide materials, energy conversion sources, semiconducting based solar cells and luminescent materials. Among all oxide based materials, SnO_2 can be treated as a unique material due to its wide variety of properties like low electrical resistance and high optical transparency in the visible region. Due to its significant properties, SnO_2 can also be used in wide variety of applications such as gas sensors, LEDs, solar cells, and optoelectronic devices [6]. SnO_2 can be treated as the host material, because the bond formation and the coexistence between tin interstitials and oxygen vacancies help in the improvement of transport of ions and optical properties. Doping with different metal oxides in SnO_2 nanostructures can improve the good optical transparency and electrical conductivity [7]. The 3d transition metal ions as dopants with open d-shell electronic configurations have various physical properties. To obtain good quality films, iron is used as one of the major source of elements for display devices. By doping Fe^{3+} ions in SnO_2 thin films, one-dimensional structure was formed due to the presence of oxygen vacancies in SnO_2. The oxygen vacancy has a great influence on the physical and chemical properties. Usually semiconductor oxide hosts are incorporated with small concentrations of activator ions, like transition (3d) or rare-earth (4f) metals. The absorption and emission bands of activators are controlled by changing the crystal field or the covalence (the activators have excitation energy levels that can be excited by direct excitation or by energy transfer from the host and then emission from the excitation states are subsequently observed) depending on site symmetry and coordination number of activator ions. Among the 3d transition metal ions, Fe^{3+} ions can show an efficient luminescence property.

SnO_2 thin films can be fabricated by using various techniques, like, chemical vapor deposition [8], sputtering [9], sol-gel [10], reactive evaporation [11], pulsed laser ablation [12], and spray pyrolysis [13]. Among these, spray pyrolysis is one of the most appropriate methods because of its facile, simplicity, low cost, easy to add doping materials and the possibility of varying the film properties by changing composition of starting solution [14]. In the present study, Fe^{3+} doped (0.01 mol %) SnO_2 thin films were prepared by using a chemical spray pyrolysis method. The as-prepared thin films were characterized by powder X-ray diffraction (XRD), optical and electron paramagnetic resonance (EPR) techniques to collect the information about the crystal structure and the site symmetry of doped Fe^{3+} ions in the SnO_2 lattice.

2. Experimental

2.1. Synthesis

All the chemicals and reagents in this experiment were of analytical grade and used without further purification. Here, Fe^{3+} doped SnO_2 thin films were synthesized by using chemical spray pyrolysis method. A spray solution was prepared by mixing 0.1 M aqueous solutions of SnO_2 and Fe_2O_3 (0.01 mol %) using magnetic stirrer. The automated spray solution was then transferred to the hot substrate kept at the normalized deposition temperature 673 K using filtered air as carrier gas at a flow rate normalized to ~ 1.8 ml/min. To prevent the substrate from excessive cooling, the prepared solution was sprayed on the substrate for 10 s with 15 s intervals. The films deposited on micro-glass slides were first cleaned with detergent water and then dipped in acetone.

2.2. Characterization

The as-prepared samples were characterized by powder XRD pattern using PANalytical Xpert Pro diffractometer with CuKα radiation (λ = 0.15405 nm). The optical absorption spectrum was recorded at room temperature using JASCO V-670 spectrophotometer in the wavelength ranging from 200 to 1400 nm. The EPR spectrum was obtained at room temperature on JEOL JES-FA series X-band EPR spectrometer having 100 kHz field modulation.

3. Results and Discussion

3.1. Powder X-ray diffraction studies

Fig. 1 shows the powder XRD pattern of Fe^{3+} doped SnO_2 thin films. The obtained XRD pattern of the as-prepared sample is in good agreement with the standard JCPDS file No. 41-1445 [15]. From the diffraction data, the as-prepared sample is indexed to a tetragonal rutile phase of SnO_2 with a space group of $P4_2/mnm$ and the corresponding lattice cell parameters are measured as a = b = 0.473 nm and c = 0.318 nm [16].

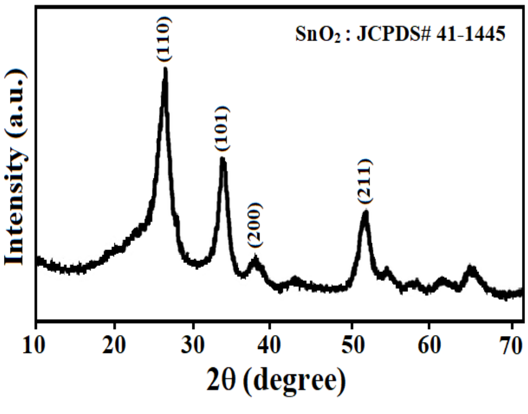

Fig. 1. Powder XRD pattern of Fe^{3+} doped SnO_2 thin films

From the analysis of the XRD pattern, it is clearly observed that the prepared sample is crystalline in nature [17]. XRD pattern shows that the prepared sample grows along the preferred orientation of (110) plane, which resembles the rutile phase of SnO_2 and the remaining planes such as (101), (200) and (211) were also detected with significant intensities [18]. The average crystallite size of the as-prepared sample is calculated by using Debye-Scherrer's formula,

$$D = (k\lambda/\beta\cos\theta)$$

where k is a constant (about 0.9), λ is the wavelength of X-ray, β is the full width at half maximum (FWHM) of the diffraction peak, and θ is the diffraction angle [19]. Based on the value of FWHM, the average crystallite size of the as-prepared sample is found to be around 23 nm, which is in the order of nano-size.

3.2. Optical absorption studies

The Fe^{3+} has an electronic configuration of [Ar] $3d^5$ equivalent to a half filled d-shell and it is predominantly most stable state of iron. The ground state of d^5 ions is ^6S which transforms into $^6A_{1g}$ state in the field of any symmetry and it is same for both octahedral and tetrahedral fields. It does not split by the effect of crystal field and hence all the transitions are spin forbidden and appear with less intensity. In the excited state it gives rise to quartet (^4P, ^4D, ^4F, ^4G) and doublet (^2S, ^2P, ^2D, ^2F, ^2H) terms. Of the above terms $^6A_{1g}$ lies lowest according to Hund's rule. It corresponds to the strong field configuration $t^3_{2g}e_g^2$. In a weak crystal field, the lower quartet terms transform as follows: $^6S \rightarrow {}^6A_{1g}$, $^4G \rightarrow {}^4T_{1g} + {}^4T_{2g} + {}^4E_g + {}^4A_{1g}$, $^4D \rightarrow {}^4T_{2g} + {}^4E_g$, $^4P \rightarrow {}^4T_{1g}$. The transitions from $^6A_1$ to $^4T_1$ and $^4T_2$ depend on the crystal field strength Dq, whereas the other bands are independent of Dq. However, the crystal field parameters in the two cases are essentially different. The Dq values in the two cases are related as $Dq_{tet} = 4/9\ Dq_{oct}$ [20].

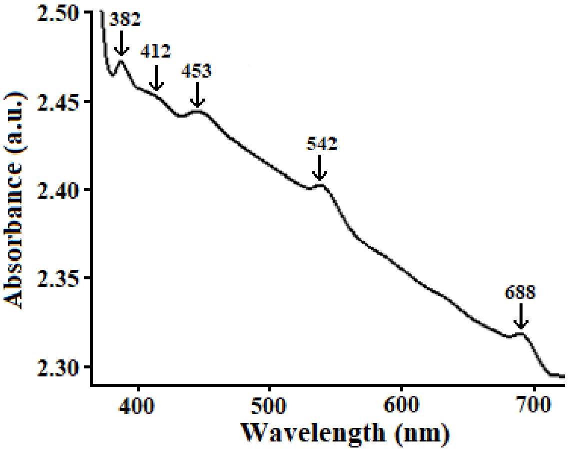

Fig. 2. Optical absorption spectrum of Fe^{3+} doped SnO_2 thin films

Fig. 2 shows the optical absorption spectrum of Fe^{3+} doped SnO_2 thin films in the region of 360-700 nm at room temperature. The absorption bands obtained in the Fig. 2 are assigned to various transitions of Fe^{3+} in the octahedral site symmetry. The bands at around 382 (26178 cm^{-1}), 412 (24271 cm^{-1}), 453 (22075 cm^{-1}), 542 (18450 cm^{-1}) and 688 (14535 cm^{-1}) nm are attributed to the transitions $^6A_{1g}(S) \rightarrow {}^4E_g(D)$, $^6A_{1g}(S) \rightarrow {}^4T_{2g}(D)$, $^6A_{1g}(S) \rightarrow {}^4A_{1g}(G)+{}^4E_g(G)$, $^6A_{1g}(S) \rightarrow {}^4T_{2g}(G)$ and $^6A_{1g}(S) \rightarrow {}^4T_{1g}(G)$ respectively.

The energy matrices of d^5 configuration are solved with Tree's correction factor (α = 90 cm^{-1}) [21], the evaluated crystal field (Dq) and interelectronic repulsion (B and C) parameters are Dq = 925, B = 700 and C = 2750 cm^{-1}. The evaluated parameters are in good agreement with the observed absorption data. These values suggest that the doped Fe^{3+} ions are in distorted octahedral site symmetry with the host lattice. The observed band head data and the calculated values are listed in Table 1.

Table 1. Optical band positions, crystal field and inter-electronic repulsion parameters of Fe^{3+} doped SnO_2 thin films

Transitions from $^6A_{1g}$ (S) ↓	**Wavelength (nm)**	**Wave number (cm^{-1})**		**Dq (cm^{-1})**	**B (cm^{-1})**	**C (cm^{-1})**
		Observed	**Calculated**			
$^4E_g(D)$	382	26178	26169	925	700	2750
$^4T_{2g}(D)$	412	24271	24318			
$^4A_{1g}(G)+{}^4E_g(G)$	453	22075	22066			
$^4T_{2g}(G)$	542	18450	18437			
$^4T_{1g}(G)$	688	14535	14578			

3.3. EPR studies

Fig. 3 shows the EPR spectrum of Fe^{3+} doped SnO_2 thin films at room temperature. Since the iron ions belong to d^5 configuration with ^6S ground state in the free ion and there is no spin-orbit interaction, g value is expected to lie very near to free ion value of 2.0023. In perfect T_d or O_h, i.e. cubic ligand fields, only one signal appears at g = 2.0 in the X-band EPR spectrum. The orbital angular momentum is zero for Fe^{3+} and therefore, the EPR spectrum can be observed even at room temperature. The EPR spectrum exhibits a signal at around g = 2.07, which can be attributed to iron ions into the host lattice at distorted octahedral site symmetry [22]. The features of the EPR spectrum can be qualitatively explained as follows: resonance peak for Fe^{3+} at around g = 2.07 can only occur if Fe^{3+} is located in a site where crystal field interaction energy is less than the magnetic Zeeman energy and arises due to isolated Fe^{3+}. From these results, the site symmetry of Fe^{3+} in host lattice is identified as an octahedral site symmetry and the same is also confirmed from the optical absorption study.

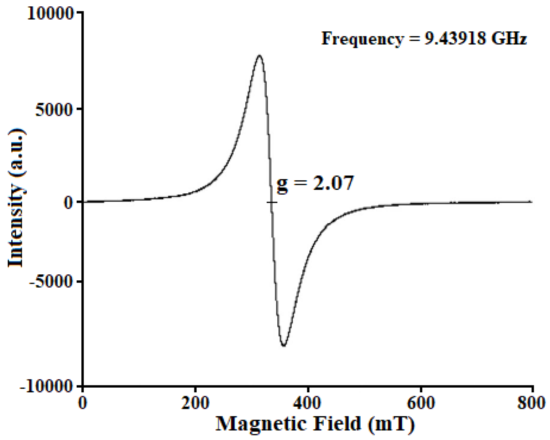

Fig. 3. EPR spectrum of Fe^{3+} doped SnO_2 thin films

4. Conclusion

In summary, Fe^{3+} doped SnO_2 thin films were successfully prepared by chemical spray pyrolysis method. From the powder XRD studies, the crystal system was indexed to a tetragonal rutile phase and the corresponding lattice cell parameters were evaluated.

The evaluated average crystallite size of the as-prepared sample was in the order of nano-scale. The optical absorption spectrum showed five characteristic bands and revealed the doped Fe^{3+} ions were in the distorted octahedral site symmetry of the SnO_2 lattice. This was also established from the EPR study, which showed a strong resonance signal at around g = 2.07, which was also a further evidence for the octahedral symmetry of Fe^{3+} ions in the host lattice.

References

[1] M. A. Manal, H. S. Mahdi, I. Sabah, Arch. Appl. Sci. Res. **4**, 1279 (2012).

[2] H. J. Jung, R. Koutavarapu, S. Lee, J. H. Kim, H. C. Choi, M. Y. Choi, J. Alloys Compd. **735**, 2058 (2018).

[3] L. Lin, J. Huang, X. Li, M.A. Abass, S. Zhang, Appl. Catal. B **203**, 615 (2017).

[4] L. P. Chikhale, F. I. Shaikh, I. S. Mulla, S. S. Suryavanshi, J. Mater. Sci. Mater. Electron. **28**, 12063 (2017).

[5] V. Geraldo, J. Eur. Ceram. Soc. **25**, 2825 (2005).

[6] M. Batzill, U. Diebold, Prog. Surf. Sci. **79**, 47 (2005).

[7] A. B. Bhise, J. Cryst. Growth **307**, 87 (2007).

[8] X. Feng, J. Ma, F. Yang, F. Ji, C. Luan, Mater. Lett. **62**, 1809 (2008).

[9] S. Boycheva, A.K. Sytchkova, M.L. Grilli, A. Piegari, Thin Solid Films **515**, 8469 (2007).

[10] Emerson A. Floriano, Luis V. A. Scalvi, Margarida J. Saeki, Julio R. Sambrano, J. Phys. Chem. A **118**, 5857 (2014).

[11] P. Patel, A. Karmakar, J. Chetan, R. P. Jayesh, Proc. Engg. **51**, 473 (2013).

[12] S. Kumar, R. S. Chauhan, G. Panchal, C. P. Singh, T. A. Dar, D. M. Phase, R. J. Choudhary, J. Appl. Phys. **122**, 125301 (2017).

[13] M. M. Bagheri-Mohagheghi, N. Shahtahmasebi, M. R. Alinejad, A. Youssefi, M. Shokooh-Saremi, Solid State Sci. **11**, 233 (2009).

[14] G Korotcenkov, V. Brinzari, I. Boris, J. Mater. Sci. **43**, 2761 (2008).

[15] N. V. Toan, N. V. Chien, N. V. Duy, H. S. Hong, H. Nguyen, N. D. Hoa, N. V. Ieu, J. Hazar. Mater. **301**, 433 (2016).

[16] M. Yuasa, T. Masaki, T. Kida, K. Shimanoe, N. Yamazoe, Sens. Actuators B: Chem. **136**, 99 (2009)

[17] K. Galatsis, L. Cukrov, W. Wlodarski, P. McCormick, K. Kalantar-zadeh, E. Comini, G Sberveglieri, Sens. Actuators B **93**, 562 (2003).

[15] S. P. Choudhurya, S. D. Gunjal, N. Kumari, K. D. Diwate, K.C. Mohite, A. Bhattacharjee, Mater. Today: Proc. **3**, 1609 (2016).

[18] B. Babu, G Rama Sundari, K. Ravindranadh, M. Rajesh Yadav, R.V.S.S.N. Ravikumar, J. Mag. Mag. Mater. **372**, 79 (2014).

[19] K. Ravindranadh, B. Babu, Ch. Venkata Reddy, Jaesool Shim, M.C. Rao, R. V. S. S. N. Ravikumar, Appl. Mag. Reson. **46**, 1 (2015).

[20] W. Low, G. Rosengarten, J. Mol. Spectro. **12**, 319 (1964).

[21] V. Pushpa Manjari, Ch. Rama Krishna, Ch. Venkata Reddy, Sk. Muntaz Begum, Y. P. Reddy, R. V. S. S. N. Ravikumar, J. Lumin. **145**, 324 (2014).

[22] C.R. Kurkjian, E.A. Sigety, Phys. Chem. Glasses **9**, 73 (1968).

---

*Corresponding author: raomc72@gmail.com